Design of a deviation information detection mechanism for sugar beet harvesters based on agricultural machinery and agronomy integration

Shenying Wang[1,2], Jinbo Pan[1,2], Qiang Xiao[4], Zhaoyan You[1], Jianmei Li[5], Xuemei Gao[1*], Shengshi Xie[3*]

(1. *Nanjing Institute of Agricultural Mechanization, Ministry of Agriculture and Rural Affairs, Nanjing 210014, China*;
2. *College of Mechanical and Electrical Engineering, Xinjiang Agricultural University, Urumqi 830052, China*;
3. *College of Mechanical and Electrical Engineering, Inner Mongolia Agricultural University, Hohhot 010018, China*;
4. *Inner Mongolia Autonomous Region Agricultural and Animal Husbandry Technology Promotion Center, Hohhot 010000, China*;
5. *Agricultural and Animal Husbandry Technology Promotion Center in Linxi County, Chifeng 025250, China*)

Abstract: To address large geometric shape differences, poor ridge distribution straightness, and the uncertain spatial distribution of beet roots during the harvesting period, as well as damage caused by the inaccurate row correction detection mechanisms of combine harvesters, this study conducts a design analysis and performance tests of deviation information detection mechanisms based on the integration of agricultural machinery and agronomy. The agronomic process of mechanized sugar beet production was analyzed, the geometric dimensions of root tubers under typical planting patterns of typical varieties in main sugar beet production areas were measured, and a three-dimensional geometric model of beet root tubers was established. A device for measuring ridge shape and root tuber distribution was designed, and agronomic parameters during the harvesting period, such as plant spacing, ridge height, unearthed height, and deviation distance of beet root tubers, were measured and analyzed. A spatial model of ridge shape and beet root tuber growth distribution on the ridge during harvesting was established. The overall structure of the deviation information detection mechanism was analyzed and designed, and the structural forms and key parameters of key mechanisms, such as left–right swing detection and up–down floating profiling, were designed on the basis of agronomic parameter analysis. Using the missed detection rate as the evaluation index, field performance tests of the deviation information detection mechanism were conducted. The results revealed that when the average forward speed of the harvester was 0.84 m/s, the average missed detection rate of the deviation information detection mechanism was 0.56%. This method has high adaptability and detection accuracy and achieves a high level of integration for agricultural machinery (detection spatial region of the detection mechanism) and agronomy (beet root distribution spatial region). This study provides a technical basis and methodological reference for improving the quality and efficiency of automatic row correction combined with harvesting operations for crops such as sugar beets.

Keywords: sugar beets, harvesting, automatic row flow, deviation information detection, agricultural machinery and agronomy integration

DOI: 10.25165/j.ijabe.20261901.10135

Citation: Wang S Y, Pan J B, Xiao Q, You Z Y, Li J M, Gao X M, et al. Design of a deviation information detection mechanism for sugar beet harvesters based on agricultural machinery and agronomy integration. Int J Agric & Biol Eng, 2026; 19(1): 120–131.

1 Introduction

Sugar beets are the second largest sugar raw material worldwide, and more than 40 countries grow sugar beets, which are distributed mainly between 30°-63°N. According to 2022 FAO (Food and Agriculture Organization of the United Nations) statistics, the global sugar beet planting and harvesting area reached 4 -295 160 hm^2, and the total yield reached 260 998 Mt. The top 10 countries in terms of harvested area are Russia (1 004 043 hm^2), the United States of America (460 170 hm^2), France (401 610 hm^2), Germany (396 300 hm^2), Turkey (274 524 hm^2), Egypt (253 825 hm^2), Poland (221 770 hm^2), Ukraine (183 800 hm^2), China (176 400 hm^2), and Belarus (94 000 hm^2).

In China, sugar beet cultivation is mainly distributed in the three northern regions north of latitude 40°, mainly Heilongjiang, Xinjiang, and Inner Mongolia, accounting for 75% to 90% of the country's planting area. In 2022, the planting area of sugar beets in China reached 176,400 hm^2, with a yield of 8 933 200 t. The main production areas of sugar beets in China mostly adopt the production mode of single ridge and single row ridge transplanting. However, owing to the lack of technical specifications and

Received date: 2025-08-26 **Accepted date:** 2026-01-14

Biographies: Shenying Wang, PhD, Associate Researcher, research interest: integration of electromechanical and hydraulic technology for agricultural equipment, Email: wangshenying@caas.cn; **Jinbo Pan**, MS candidate, research interest: agricultural mechanization, Email: 2157977186@qq.com; **Qiang Xiao**, MS, Agronomist, research interest: technology promotion of industrial crop, Email: 327531828@qq.com; **Zhaoyan You**, MS, Assistant Researcher, research interest: agricultural equipment mechanization, Email: 1275306672@qq.com; **Jianmei Li**, BS, Promotion Researcher, research interest: promotion of economic crop technology, Email: lxdjz666@163.com.

***Corresponding author: Xuemei Gao**, MS, Assistant Researcher, research interest: agricultural mechanization. Nanjing Institute of Agricultural Mechanization, MARA, Nanjing 210014, China. Tel: +86-18761856717, Email: gaoxuemei@caas.cn; **Shengshi Xie**, PhD, Associate Professor, research interest: crop harvesting equipment technology. College of Mechanical and Electrical Engineering, Inner Mongolia Agricultural University, Hohhot 010018, China. Tel: +86-25-84346078, Email: xieshengshi@163.com.

standards for transplanting, differences in varieties and regions, uncertainties in weather conditions such as wind and rain, and the influence of field management machinery such as tillage and fertilization during the harvesting period, prominent problems exist such as unequal planting row spacing, large differences in geometric shape, indefinite spatial distribution (spatial area distributed in the direction of up and down, left and right, and front and back), and poor straightness in ridge distribution[1].

Combine harvesting has become the main harvesting method for sugar beets because of its high efficiency. At present, the automation level of sugar beet combine harvesting machinery in China is relatively low. Deviations in the direction of the digging shovel during excavation and harvesting operations can lead to missed extraction, insufficient excavation, or root tuber damage, requiring manual excavation and resulting in losses and low efficiency. At the same time, to reduce leakage, drivers need to highly concentrate on harvesting and adjust the direction of travel in real time, which is labor intensive. Harvesting performance is easily affected by human factors, making effective and efficient harvesting operations difficult[2]. Therefore, it is necessary to carry out beet excavation by following rows and correcting deviations when the beets are harvested. The detection of sugar beet tubers is a prerequisite for achieving automatic row following and excavation, and the detection accuracy is affected by both the detection mechanism and the spatial distribution of sugar beet tubers. Therefore, studying the degree of overlap between the spatial region of the detection mechanism and the growth distribution of sugar beet roots in the field is highly important for improving the performance of automatic row excavation to integrate agricultural machinery and agronomy in detail[3]. Multi-sensor information fusion is the core direction to improve the accuracy of field environmental perception, which compensates for the limitations of single perception by complementing information from different sensors. Zhang et al.[4] pointed out in their review that the complementarity of sensor characteristics and multi-dimensional data fusion are key to solving complex farmland perception problems, which is highly consistent with the design idea of collaborative perception based on agronomic parameters and sensor signals in this study.

European and American countries have previously studied the mechanization of sugar beet harvesting. Marchant et al.[5] designed a traction-type sugar beet combine harvester by configuring side discharge bins, lifting wheels, and a lifting chain on a universal chassis. An automatic depth-limiting steering system was designed by driving a hydraulic servo system through a pair of antenna rods mounted on the sugar beet row; a mechanical contact method for detecting sugar beet tubers was proposed for the first time. Billington[6] designed a rotating cylindrical inclined bar top cutter to address the waste problem caused by the disposal of the crown interior, which can still be used above the horizontal cutting plane of sugar beets. O'Dogherty[7] established a geometric model of the beet top cutting mechanism on the basis of field measurements and studied the cause of inaccurate crown sensing of the top detection wheel. Ivancan et al.[8] studied the factors affecting the performance and quality of sugar beet combine harvesters and reported that agronomic parameters such as uniform row spacing and crown height differences between two adjacent beets had a decisive effect on operation quality. Tillett et al.[9] developed a high-speed automatic guidance system for inter-row weed control in sugar beets based on their research on inter-row weed control in grains. Bulgakov et al.[10] studied agronomic parameters such as the height distribution of beet root crowns protruding from the soil surface to avoid losses caused by excessive cutting of beet root crowns and excessive stubble of stems and leaves. Ospina et al.[11] designed a machine vision method that can simultaneously perform mapping and crop line detection via a new camera developed using a real-time kinematic global positioning system (RTK-GPS), a fiber optic gyroscope (FOG), and Fujifilm. Tsukor et al.[12] developed and optimized a noncontact sensor control system for automatic row following and depth limiting of sugar beet harvesters via 3D ToF camera technology. LiDAR has also shown excellent performance in farmland navigation; Yang et al.[13] achieved a field road extraction accuracy of over 98% based on LiDAR point cloud data mounted on agricultural vehicles, verifying the reliability of noncontact sensors in field navigation. However, during sugar beet harvesting, there are many stem and leaf fragments around the root tubers, and the ridge surface is uneven, making such noncontact detection prone to interference. Ivanetz et al.[14] conducted virtual testing of the excavation components of a VHP NAS sugar beet harvester in Belarus via LS-DYNA software, simulating and analyzing the effects of the soil type, excavation shovel opening angle, and operating speed on the excavation process. Bulgakov et al.[15,16] studied the effect of vibration on the working quality of a tractor front-mounted sugar beet leaf harvester and established a mathematical relationship between the beet root crown shape and the cutting loss, as well as a nonlinear differential equation for the vibration of the top cutting mechanism in the longitudinal vertical plane. In other crop row detection fields, computer vision technology is commonly used. Examples include grapevine row detection, accurate detection and removal of weeds between crop rows, and sugarcane row detection along with gap measurement[17-21].

Beet harvesters have been researched and developed in China for many years. In recent years, the author and his team proposed an active automatic row-following digging and harvesting method, designed a beet automatic row-following detection mechanism by using a mechanical contact detection rod and angle sensor, simulated and analyzed its motion process, and developed a scientific research prototype of a traction-type sugar beet combine harvester[22]. The top cutting device, conveying device, and automatic row following system were previously studied[23]. Wang et al.[24-26] designed a hydraulic row guide device and top cutting device for excavating beet harvesting machinery, analyzed the force and motion characteristics of the guide mechanism, established a dynamic equation for the guide rod, and defined the key structural parameters affecting the working quality through kinematic and mechanical analyses of the profiling top cutting device. Yang et al.[27] adopted the mechanical contact detection method and installed a left and right contact rod and angle sensor on the front of the digging shovel of a tracked peanut combine harvester, achieving automatic sensing of the digging angle. By controlling the hydraulic cylinder to drive the excavator structure to move left and right along a transverse guide rail, automatic row-following harvesting was achieved. Hu et al.[28] designed an automatic row boundary detection method for corn combine harvesters using laser radar as a distance sensor. Li et al.[29] designed a mechanical contact-type deviation information extraction mechanism using a 4UGS2 double-row potato harvester as the carrier and a ridge-shaped section direction as the automatic row-following target, as shown in Figure 1. Han et al.[30] studied an automatic guidance control system based on a slip estimation path tracking algorithm using RTK-GPS and inertial

measurement unit (IMU) technology to address the problem of low guidance accuracy caused by the slipping of South Korean automatically guided agricultural vehicles due to wet rice fields. Zhang et al.[31] designed a mechanical row-following sensor for the automatic perception of the navigation environment of corn harvesters, as shown in Figure 2. In the mechanized production of other crops, vision technology has been adopted for the detection of crop rows[32-35]. Luo et al. developed a rapid and robust detection method for detecting the harvesting edge for multiple crops based on stereo vision, and in order to improve the processing speed and keep the crop harvesting edge within the target region, they developed a dynamic ROI (region of interest) extraction algorithm based on HSV (hue, saturation, and value) space scanning[36].

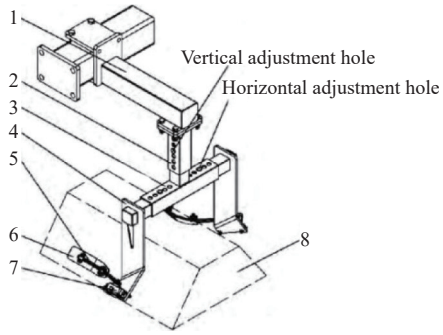

1. Rack installation base; 2. Vertical support; 3. Horizontal support; 4. Left and right connecting frame; 5. Sensor contact rod; 6. Arc detection plate; 7. Angle sensor; 8. Ridge

Figure 1 Schematic diagram of the deviation information extraction mechanism

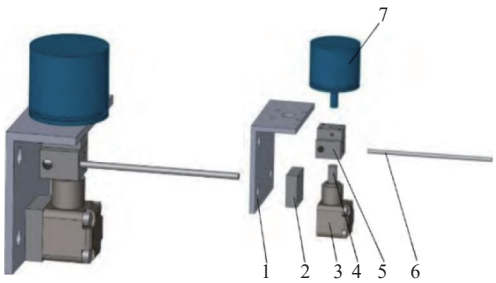

1. Installation base; 2. Cushion block; 3. Shell; 4. Shaft; 5. Connection block; 6. Contact rod; 7. Angle sensor

Figure 2 Structural diagram of the mechanical row-following sensor for a corn harvester

In summary, research on crop row correction detection methods has focused mainly on mechanical contact, LiDAR, or visual recognition. Owing to the preharvest leaf cutting and topping operation of sugar beets, there are scattered fragments of stems, leaves, and roots (similar in color to the roots) around the sugar beet tubers, and the surface is uneven, making it difficult to apply visual recognition and laser radar detection methods during sugar beet harvesting. The mechanical contact detection method can be applied to detect deviation information in sugar beets. Since the process and quality of the harvesting operation for row correction are affected by the growth conditions of the beets in the field, research on the process of beet harvesting has focused mostly on the movement of the digging mechanism, the row-guiding mechanism, and the top cutting mechanism, and only a few reports on the agronomic parameters have been published, so the accuracy of the mechanical contact detection method is not high.

In view of the above problems, the author proposes the design and experimental research of an automatic row-following deviation information detection mechanism for beet harvesters on the basis of integrating agricultural machinery and agronomy. The measurement and modeling of the agronomic characteristics of sugar beets during the harvesting period, such as their geometric shapes, spatial distributions, and ridge shapes, are studied; the deviation information detection mechanism structure and key parameters are designed to improve the degree of overlap between the detection mechanism and spatial region (the spatial region formed by the structure of the detection rod and its movement trajectory); and the spatial region of sugar beet root distribution is adjusted to avoid missed detections, thus improving the adaptability and accuracy of the detection mechanism and laying a foundation for improving the quality and efficiency of automatic row-following and correction harvesting operations of sugar beet combine harvesters.

2 Agronomic mechanized production process for beets

The mechanized production of sugar beets mainly includes processes such as ridging, transplanting, field management, leaf cutting, deviation information detection, and row-following excavation. First, an integrated machine for rotary tillage, ridge raising, fertilization, and drip irrigation belt laying is used to complete ridge raising and drip irrigation belt laying for sugar beets. Different machines can also be applied to link rotary tilling, ridging, laying drip irrigation belts, and fertilization step by step, but the former has a high degree of mechanization and saves time and labor. In the middle stage of sugar beet growth, general field management machinery can be used to complete field management operations such as loosening soil, weeding, fertilizing, and spraying pesticides. After the beet is mature, the beet leaves are crushed and returned to the field via a sugar beet leaf-cutting machine, and the tops of the beet roots are cut off. A sugar beet combine harvester is then used to excavate and harvest the remaining sugar beet tubers. During the combine harvesting of sugar beets, the root deviation of beets should be detected first, and then combine harvest operations such as row-following excavation, soil removal, and root tuber collection should be carried out. The specific agronomic process is shown in Figure 3.

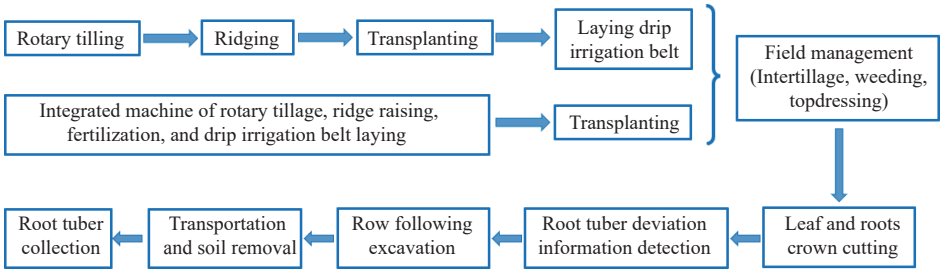

Figure 3 Agronomic mechanized production process for beets

3 Determining and modeling the agronomic field characteristics of sugar beets during the harvesting period

3.1 Determining and modeling the geometric shapes of sugar beet root tubers

The size, shape, and other geometric features of sugar beet tubers affect the structural form and operational performance of the detection mechanism. A beet is a fleshy tuber formed by the enlargement of the taproot, mainly in the shape of a wedge, cone, spindle, or hammer. The root tubers can be divided into three main parts: the root head, the root neck, and the root body. The root head is the top part of the root tuber, also known as the green head, which is actually a shortened stem and the growth site of the petiole and bud. The lower part of the root head is connected to the root neck, and its boundary is the growth site of the lowest layer of leaves. The root neck is under the root head, between the root head and the root body, and the upper part is bounded by the leaf marks at the lower end of the root head. The root body is the main part of the root tuber, and the root body from the lower end of the root neck to the diameter of the main root, at 1 cm in diameter, is called the root tail, as shown in Figure 4.

1. Root head 2. Root neck 3. Root body 4. Root tail

Figure 4 Beet root tuber

To mitigate the impact of the geometric shape diversity of beet roots on the design of key structural elements and parameters for deviation information detection mechanisms, a comprehensive analysis and measurement of the geometric parameters of typical beet varieties in major production areas were conducted.

3.1.1 Experimental materials and methods

Field experiments were conducted in Chahar Right Front Banner, Ulanqab city, Inner Mongolia Autonomous Region, which is a representative main production area of single ridges and single rows of sugar beets. The Chahar Right Front Banner is located at east longitude 112°48′-113°40′ and north latitude 40°41′-41°13′, is mostly cold and dry, has more wind and less rain, and has a large temperature difference between day and night. The climate is a northern temperate continental arid climate, with winters lasting as long as five months. The average annual temperature is 4.5°C, the annual precipitation is 376.1 mm, and the average annual frost-free period is 131 d.

The sugar beet variety was the Jitian series. The soil in the experimental field was semiarid grassland dark chestnut calcareous soil, and the planting mode was single ridge and single row planting.

The main test instruments and equipment used included the 4TGQ-3 sugar beet leaf cutting machine produced by Changzhou Hansen Machinery Co., Ltd. (with a supporting power of 50-70 kW, working width of 1700 mm, 3 rows of operation, and adjustable row spacing of 460-550 mm), the 4TW-3 sugar beet excavator (with a supporting power of 50-70 kW, working width of 1700 mm, and 3 rows of operation), an electronic digital Vernier caliper produced by Yantai Green Forest Tools Co., Ltd. (with a range of 300 mm, resolution of 0.01 mm, and accuracy of ±0.03 mm), and an SYJDC200 electronic digital angle ruler produced by Deqing Shengtaixin Electronic Technology Co., Ltd. (with a range of 0-360° and accuracy of 0.05°).

Other test equipment included square rulers, benchmarks, tape measures, etc.

Before measurement, a field with normal and uniform sugar beet growth was selected, five small plots were randomly selected from the field, and samples with a size of 200×200 cm^2 were randomly selected from each plot. The beet leaves were crushed and returned to the field by a 4TGQ-3 beet leaf-cutting machine, and the beet heads were cut off. Then, 4TW-3 beet excavators were used to excavate the root tubers and arrange them in a strip-like pattern. The dimensions of different parts of the sugar beet root were measured via electronic digital Vernier calipers and angle rulers, as shown in Figure 5. Statistical analysis was conducted on the measurement results via IBM SPSS 19.0 software to establish a three-dimensional model of sugar beet tubers.

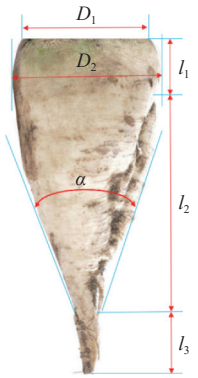

Note: l_1 is the root neck length, mm; l_2 is the root body length, mm; l_3 is the root tail length, mm; D_1 is the root neck small diameter, mm; D_2 is the root neck large diameter, i.e., the root body large diameter, mm; and α is the root body taper, (°).

Figure 5 Geometric parameters of sugar beet tubers

3.1.2 Test results and analysis

The results of the measurements and analysis are shown in Table 1 and Figure 6.

According to Table 1, the average root neck length of sugar beet tubers is 44.69 mm, with a maximum of 59.41 mm. The average length of the root body is 122.39 mm, with a maximum of 145.63 mm. The average length of the root tail is 33.55 mm, with a maximum of 49.35 mm. The average root neck small diameter is 72.17 mm, with a maximum value of 90.47 mm. The average root neck large diameter is 126.59 mm, with a maximum of 169.01 mm. The average taper of the root body is 39.20°, with a maximum of 55.57°.

According to Figure 7, the root neck length of sugar beet tubers is concentrated in the range of 30.00-60.00 mm, the root body length is concentrated in the range of 100.00-150.00 mm, the root tail length is concentrated in the range of 20.00-50.00 mm, the root neck small diameter is concentrated in the range of 50.00-95.00 mm, the root neck large diameter is concentrated in the range of 80.00-175.00 mm, and the root body taper is concentrated in the range of 25.00°-55.00°.

Table 1 Statistical results of the geometric parameter frequency of beet tuber roots

	Root neck length l_1/mm	Root body length l_2/mm	Root tail length l_3/mm	Root neck small diameter D_1/mm	Root neck large diameter D_2/mm	Root body taper α/(°)
Effective	50	50	50	50	50	50
Deficiency	0	0	0	0	0	0
Mean	44.6906	122.3874	33.5484	72.1674	126.5862	39.1956
Standard error of mean	1.170 67	1.707 70	1.184 97	1.873 79	3.780 49	1.148 76
Mid-value	44.5850	121.1200	32.9300	73.3150	129.0950	41.2200
Mode	31.33	100.44	20.10	86.48	82.27	25.49
Standard deviation	8.277 89	12.075 25	8.379 00	13.249 67	26.732 12	8.122 94
Variance	68.523	145.812	70.208	175.554	714.606	65.982
Skewness	.094	0.071	0.211	–0.286	–0.050	0.042
Standard error of skewness	0.337	0.337	0.337	0.337	0.337	0.337
Kurtosis	–1.105	–0.822	–1.019	–1.262	–1.138	–1.079
Standard error of kurtosis	0.662	0.662	.662	0.662	0.662	0.662
Range	28.08	45.19	29.25	40.09	86.74	30.08
Minimum value	31.33	100.44	20.10	50.38	82.27	25.49
Maximum value	59.41	145.63	49.35	90.47	169.01	55.57
Sum	2234.53	6119.37	1677.42	3608.37	6329.31	1959.78
Percentile 10	33.4770	104.6190	22.4280	51.4250	88.4920	28.6400
20	36.2820	111.8380	25.0560	58.1040	95.7780	29.8980
25	37.1525	114.1700	26.4050	61.0075	99.2775	32.2900
30	38.8200	115.5180	27.9000	64.5460	112.7740	33.5530
40	41.9880	117.7600	29.7340	69.3920	118.0840	35.0280
50	44.5850	121.1200	32.9300	73.3150	129.0950	41.2200
60	46.0100	126.0180	36.7560	79.1480	134.3340	42.6860
70	49.7930	129.1760	38.8640	82.8960	142.4240	44.3800
75	51.9275	130.9875	39.7875	83.9675	147.2850	45.3300
80	53.4900	136.0660	41.3780	86.2260	155.5920	46.0320
90	55.7670	139.0750	46.0020	88.5530	165.5920	51.3350

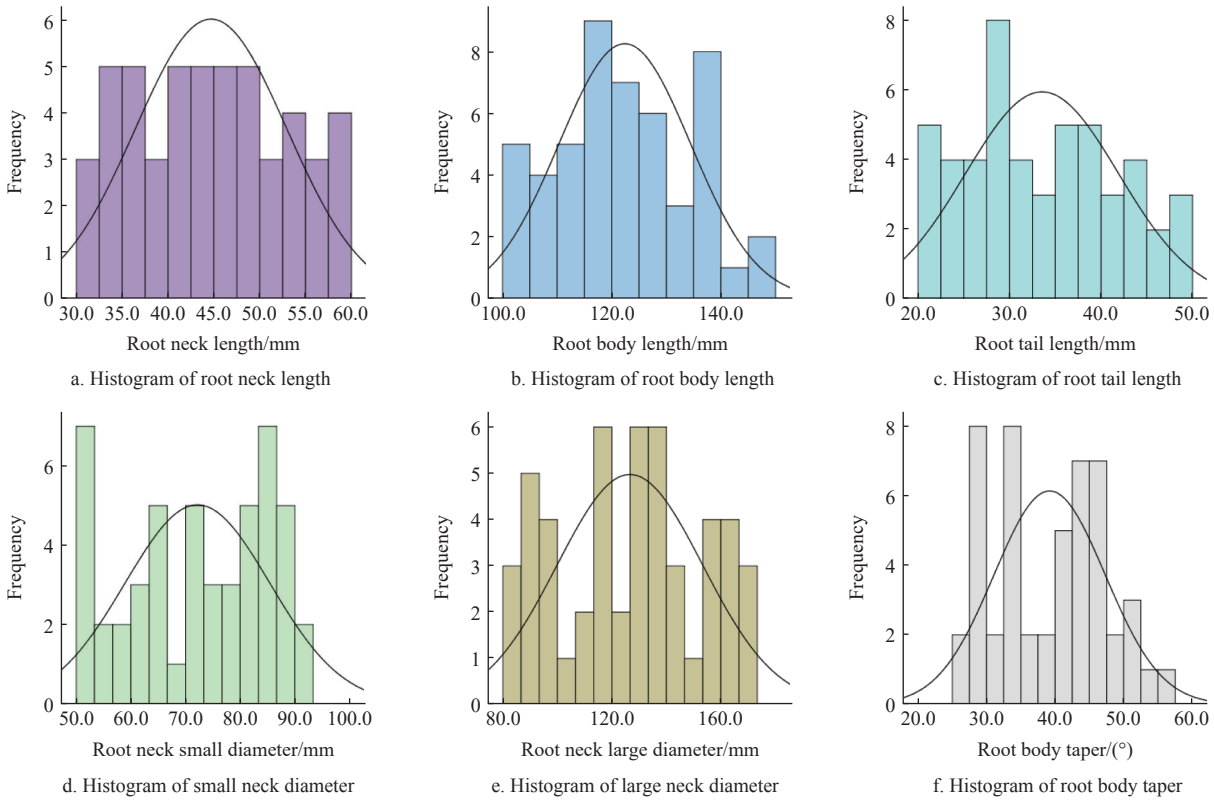

a. Histogram of root neck length b. Histogram of root body length c. Histogram of root tail length

d. Histogram of small neck diameter e. Histogram of large neck diameter f. Histogram of root body taper

Figure 6 Geometric characteristics histogram of beet root tubers

3.1.3 Modeling of beet root

On the basis of the above measurement and analysis results, the three-dimensional design software Autodesk Inventor was applied to model the four main shapes of sugar beet tubers, as shown in

Figure 7.

3.2 Spatial detection and modeling of ridge shape and root growth distribution during the harvesting period

3.2.1 Ridge shape and root distribution detection device

To detect the spatial distribution of sugar beet tubers on ridges accurately, a modular and rapid splicing ridge shape and sugar beet tuber field growth distribution detection device was developed, as shown in Figure 8. It consists of an I-frame, an angle adjustment mechanism, a ridge shape extractor combination, a rapid tightening mechanism, and a rectangular frame.

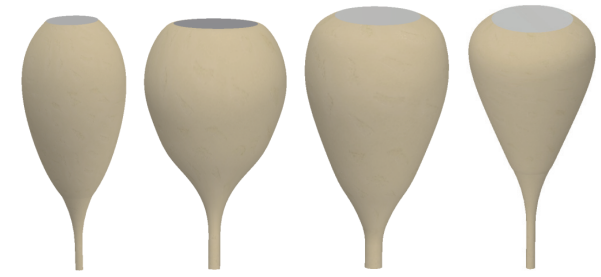

a. Spindle shape b. Hammer shape c. Cone shape d. Wedge shape

Figure 7 3D model of sugar beet root tubers

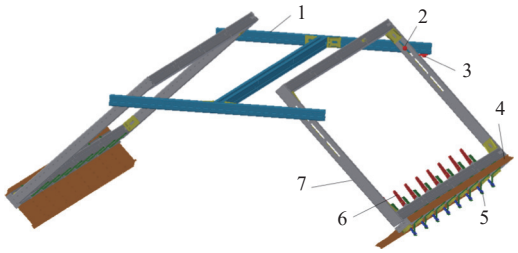

1. I-frame; 2. Locking bolt group; 3. Angle adjustment mechanism; 4. Ridge shape extractor combination; 5. Hanging ear; 6. Quick tightening mechanism; 7. Rectangular frame

Figure 8 Diagram of the ridge shape and beet root field growth distribution device

The detection device frames are all made of guide rail profiles, and two rectangular frames are symmetrically assembled with the I-frame through locking bolt sets. The hanging ear is fixed to the rectangular frame by locking bolts, and the ridge shape extractor combination is fixed to the rectangular frame by the quick tightening mechanism and hanging ear. The angle between the rectangular frame and I-frame can be changed by adjusting the angle adjusting mechanism. The short side guide rail of the rectangular frame is provided with a long waist-shaped hole to adjust the relative positions of the rectangular frame and the I-frame.

The angle adjustment mechanism consists of two sets of positioning plates, T-bolts, and self-locking nuts, as shown in Figure 9. The rectangular frame is hinged with the I-frame by the T-nut and self-locking bolt, and the positioning plate is fixed in the profile trapezoidal chute of the I-frame by the T-bolt and self-locking nut and can be moved along the chute. By adjusting the distance between the upper and lower positioning plates and the hinge point between the rectangular frame and the I-frame, the tilt angle of the rectangular frame can be adjusted. The upper and lower positioning plates can increase the overall stability of the detection device. Moreover, adjusting the position of the hinge point in the trapezoidal chute of the I-frame can adjust the width of the detection device's ridge top. By adjusting the position of the hinge point in the trapezoidal chute of the rectangular frame, the length of the ridge waist and the height of the ridge can be adjusted. Therefore, the ridge shape detection device can adapt to different ridge shapes (height, top width, bottom width, and waist length) and can also detect and shape different crop ridges in different regions.

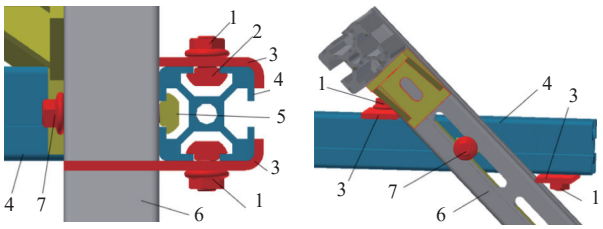

a. Front view b. Side view

1. Self-locking nut; 2. T-bolt; 3. Positioning plate; 4. I-frame; 5. T-nut; 6. Rectangular frame; 7. Self-locking bolts

Figure 9 Schematic diagram of the angle adjustment mechanism

The ridge-shaped extractor combination mainly consists of a shape extractor, a locking mechanism, and a hanging ear, as shown in Figure 10. The hanging ear is fixed in the trapezoidal chute of the rectangular frame by a T-shaped bolt group, and the locking mechanism is connected to the hanging ear through a fixed seat. The shape extractor (as shown in Figure 11) can be quickly and tightly assembled into a long strip shape through trapezoidal grooves and convex grooves at both ends, with one end being larger and the other being smaller, and clamped and fixed in the U-shaped groove of the hanging ear by the locking mechanism.

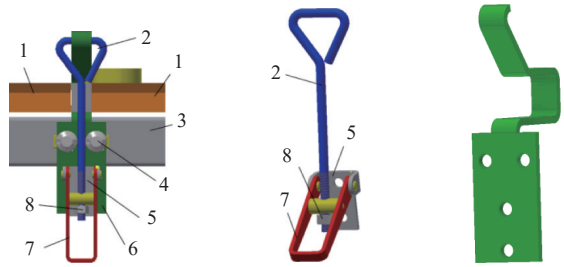

a.Overall structure b.Locking mechanism c.Hanging ear

1. Shape extractor; 2. Pull rod; 3. Rectangular frame; 4. T-bolt group; 5 Fixed seat; 6. Hanging ear; 7. Handle; 8. Nut adjustment

Figure 10 Schematic diagram of the ridge shape extractor combination

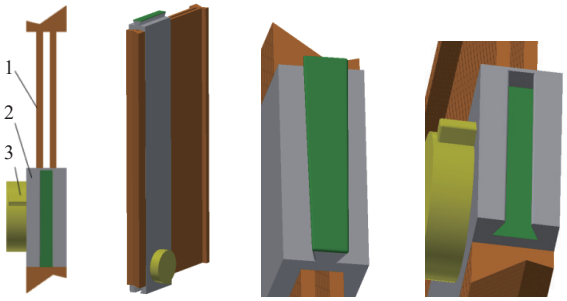

a. Structural schematic diagram b. Axial view c. Convex connection groove connection groove d. Concave connection groove

1. Shaped rack; 2. Ruler body; 3. Shaped lock

Figure 11 Schematic diagram of the ridge shape extractor

To meet the requirements of ridge shape detection devices for measuring different lengths, the long sides of the rectangular frame and I-frame are composed of multiple guide rail profiles, and their lengths can be adjusted by increasing or decreasing the number of guide rail profiles.

3.2.2 Determination of agronomic field parameters during the harvesting period

The determined sugar beet varieties, planting methods, environments and climates, main instruments and equipment, and sugar beet field selection methods are the same as those in Section 2.1.

For measurement, a 4TGQ-3 sugar beet leaf-cutting machine was first used to crush and return the beet leaves to the field, after which the green head was cut. Then, the above developed detection device was mounted on the ridge, and the I-frame was placed on the top of the ridge and closely attached to the top surface of the ridge so that the center beam of the I-frame coincided with the centerline of the sugar beet root. By measuring the distance from the sugar beet root to the center beam of the I-frame and the distance above the top surface of the ridge with a right angle ruler, the deviation distance from the center of the row and the unearthed height of the sugar beet root could be obtained. The distance between two sugar beet tubers along the central beam direction of the I-frame was measured via a square ruler, which represents the plant spacing; the distance from the bottom of the ridge to the lower plane of the I-frame was measured via a square ruler, which represents the ridge height; and the tilt angle of the two rectangular frames was adjusted according to the actual ridge shape and measured with a digital angle ruler. At the same time, the rectangular frame was parallel to the inclined surface of the actual ridge (i.e., the ridge waist), the ridge shape extractor was pressed and made perpendicular to the inclined surface of the ridge waist and closely fit, and the shape formed by the rack of the extractor was the ridge shape. The determination of field agronomic parameters is shown in Figure 12. Statistical analysis was conducted on the measurement results via IBM SPSS 19.0 software, and the results are shown in Figure 13 and Table 2.

Figure 12 Agronomic parameter measurement

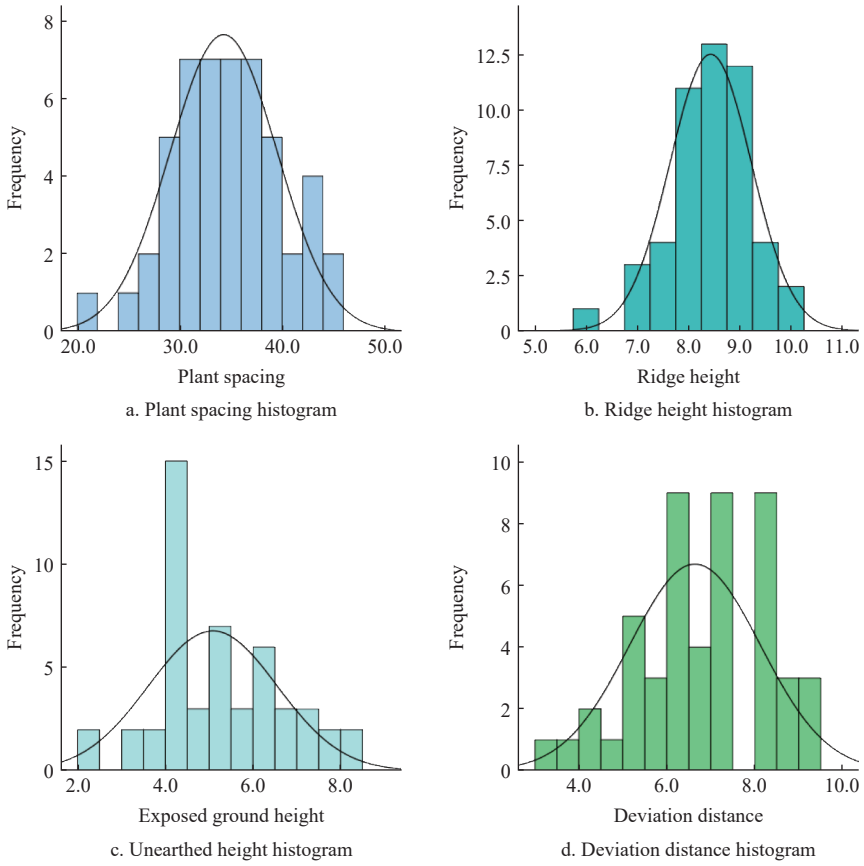

Figure 13 Histogram of sugar beet agronomic field characteristics during the harvesting period

As shown in Table 2, the mean and maximum plant spacings of the sugar beet root tubers during the harvesting period were 34.30 cm and 45.00 cm, respectively. The average ridge height was 8.43 cm, and the maximum value was 10.00 cm. The average unearthed height was 5.08 cm, with a maximum of 8.00 cm. The average deviation distance was 6.64 cm, and the maximum value was 9.00 cm.

According to Figure 13, during the harvesting period, the plant spacing of the sugar beet tubers was concentrated between 25.00-45.00 cm, the ridge height was concentrated between 7.00-10.00 cm,

the unearthed height was concentrated between 3.00-8.00 cm, and the deviation distance was concentrated between 4.00-9.00 cm.

Table 2 Statistical results of sugar beet agronomic field parameters during the harvesting period

	Plant spacing S/cm	Ridge height H_1/cm	Unearthed height H_2/cm	Deviation distance L_d/cm
N Effective	50	50	50	50
Deficiency	0	0	0	0
Mean	34.3000	8.4300	5.0826	6.6400
Standard error of mean	0.738 59	.112 49	.208 13	0.210 75
Mid-value	34.0000	8.5000	5.0000	6.8650
Mode	31.00	8.50	4.00	6.00
Standard deviation	5.222 60	0.795 46	1.471 69	1.490 20
Variance	27.276	0.633	2.166	2.221
Skewness	–0.022	–0.521	0.243	–0.397
Standard error of skewness	0.337	0.337	0.337	0.337
Kurtosis	–0.139	0.808	–0.369	–0.362
Standard error of kurtosis	0.662	0.662	0.662	0.662
Range	24.00	4.00	6.00	6.00
Minimum value	21.00	6.00	2.00	3.00
Maximum value	45.00	10.00	8.00	9.00
Sum	1715.00	421.50	254.13	332.00
Percentile 10	28.0000	7.5000	3.7810	4.5500
20	30.0000	8.0000	4.0000	5.2000
25	31.0000	8.0000	4.0000	5.8300
30	31.0000	8.0000	4.0000	6.0000
40	33.0000	8.5000	4.2800	6.1400
50	34.0000	8.5000	5.0000	6.8650
60	35.6000	8.5000	5.0300	7.0000
70	37.0000	9.0000	6.0000	7.8080
75	38.0000	9.0000	6.0000	8.0000
80	38.8000	9.0000	6.4900	8.0000
90	42.0000	9.5000	7.0000	8.5470

3.2.3 Establishment of a spatial model of ridge shape and root growth distribution

A 3D model of the ridge shape was created via the 3D design software Autodesk Inventor. On the basis of the above measurement and analysis results, the four main shapes of sugar beet tubers established above, with average sizes (Spindle shape: root neck length 35 mm, root body length 130 mm, root tail length 30 mm, root neck small diameter 60 mm, root neck large diameter 95 mm, root body taper 30°; Hammer shape: root neck length 55 mm, root body length 120 mm, root tail length 35 mm, root neck small diameter 85 mm, root neck large diameter 165 mm, root body taper 50°; Cone shape: root neck length 45 mm, root body length 140 mm, root tail length 25 mm, root neck small diameter 75 mm, root neck large diameter 125 mm, root body taper 40°; Wedge shape: root neck length 40 mm, root body length 110 mm, root tail length 45 mm, root neck small diameter 65 mm, root neck large diameter 110 mm, root body taper 35°), were placed on the ridge (with average plant spacing 35 cm, unearthed height 5 cm, deviation distance 6.5 cm), and a spatial distribution model of ridge shape and roots on the ridge was established, as shown in Figure 14.

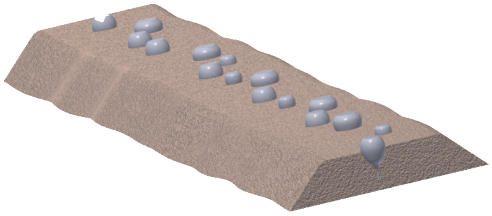

Figure 14 Spatial distribution model of ridge shapes and roots on ridges

4 Designing the deviation information detection mechanism

The typical row-following harvesting method in the main sugar beet production areas of China involves the use of a traction-type sugar beet combine harvester for row-following correction harvesting, as shown in Figure 15[37-38]. During operation, the deviation information detection mechanism senses the deviation information of the beet root tubers on the ridge and converts it into an electrical signal, which is transmitted to the controller. The controller sends out a signal to control the action of the hydraulic deviation correction actuator, driving the mechanical system of the "deviation information detection mechanism-hydraulic correction actuator-excavation mechanism" to move around points O_1 and O_2 and then driving the excavation mechanism to swing left and right for row-following harvesting.

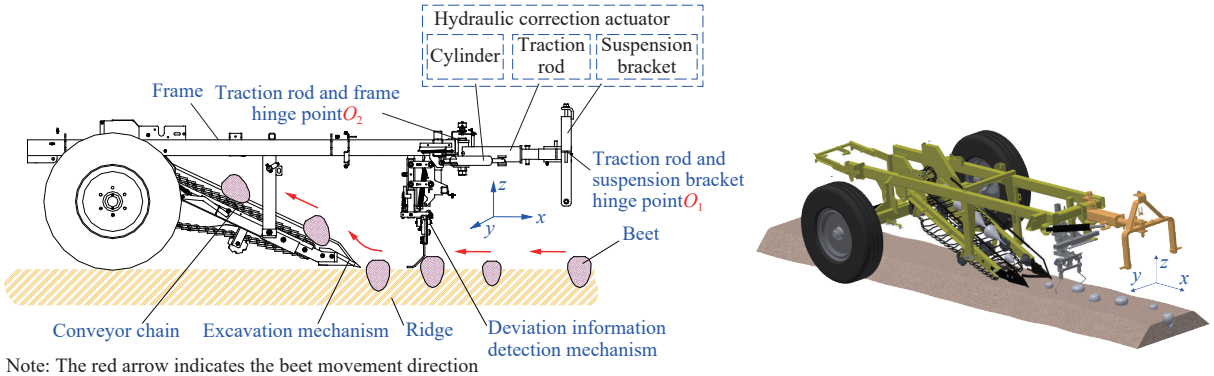

Note: The red arrow indicates the beet movement direction

a. Schematic diagram of the operation process b. 3D schematic diagram

Figure 15 Principle schematic diagram of row-following correction harvest operation

According to the above research results on the agronomic field characteristics of sugar beets, the geometric shape of sugar beet tubers and their distribution on ridges differ. To adapt to the detection of sugar beet tubers at different positions, the detection mechanism should be able to swing left and right, float up and down, and the detection spatial region of the detection mechanism (the spatial area formed by the structure of the detection mechanism and its forward movement trajectory, that is, the spatial area formed

by the shape of the detection mechanism on the *yz* plane and the movement trajectory in the *x*-axis direction) should be able to cover the spatial distribution region of sugar beet tubers.

To solve the above problems, a double parallel four-bar linkage mechanism is adopted to design the detection mechanism, as shown in Figure 16, which consists of an upper and lower profiling mechanism, a left and right swing detection mechanism, a tension spring, and a frame. The left and right swing detection mechanism is fixed on the upper and lower profiling mechanism, which is used mainly to detect the left and right positions of sugar beet tubers. The upper and lower profiling mechanism is hinged to the frame through bearings and suspended on the frame through tension springs, which are used mainly to detect the upper and lower positions of the ridge top surface and drive the left and right swing detection mechanisms to float up and down, preventing the detection mechanism from becoming stuck in the soil and affecting smooth operation.

4.1 Detection mechanism

The detection mechanism is mainly composed of a mounting frame, detection rods, a signal conversion mechanism, a reset limit plate, a swing arm, and a reset spring, as shown in Figure 17a. During operation, the detection rod senses the left and right deviation of the beet root on the ridge, drives the swing arm to rotate, and converts the left and right displacement of the detection rod into angular changes through the signal conversion mechanism (as shown in Figure 17b), which is then converted into digital signals and transmitted to the controller to control the hydraulic steering actuator, achieving an automatic row-following function.

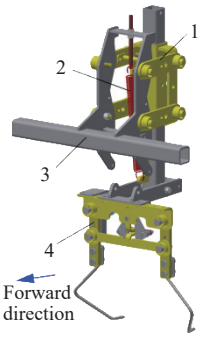

1. Upper and lower profiling mechanism; 2. Tension spring; 3. Frame; 4. Left and right swing detection mechanism

Figure 16 Structural diagram of deviation information detection organization

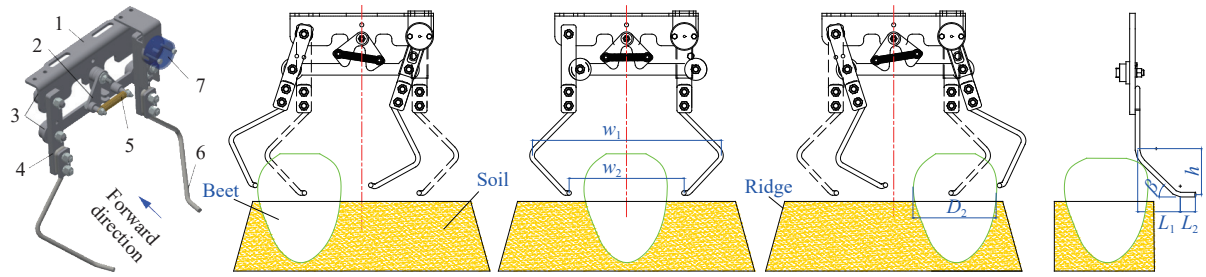

a. Structural schematic diagram b. Operational diagram

1. Mounting frame; 2. Reset limit plate; 3. Bearing; 4. Swing arm; 5. Reset spring; 6. Detection rod; 7. Signal conversion mechanism

Figure 17 Structure and operation diagram of the detection mechanism

The detection rod is the first part that comes into contact with the sugar beet root, and detecting the sugar beet root smoothly without omission is the foundation and prerequisite for achieving accurate detection. Therefore, the detection rod adopts a structural form of "double character 'V' + horizontal extension", as shown in Figures 17 and 18. The upper part of the detection rod is perpendicular to the ground and gradually increases downward, forming a vertical "V" shape. The lower part tilts toward the ground and gradually decreases downward and inward, forming a tilted inverted "V" shape. The "V"-shaped detection rod is not only beneficial for capturing deviated sugar beet roots inside the detection rod but also improves the passing smoothness of the detection mechanism. The tail is parallel to the ground and adopts a "horizontal extension" structural form, which is conducive for contact between the detection rod and the ground while preventing the detection rod from sinking into the soil.

To detect all deviated sugar beet tubers, the entry width of the detection rod w_1 should meet the following conditions:

$$w_1 \geq 2(L_{dmax}+D_{2max}/2) \quad (1)$$

where, w_1 is the entry width of the detection rod, mm; L_{dmax} is the maximum deviation distance of the sugar beet root, mm; and D_{2max} is the maximum diameter of the beet root neck, mm.

According to the measurement results of the agronomic characteristics mentioned above, L_{dmax}=90 mm and D_{2max} = 169.01 mm. When the above data are substituted into Equation (1), $w_1 \geq$ 349.01 mm. To ensure that the sugar beet root with the largest root neck and deviation distance can easily enter the interior of the detection rod, the extension width of the detection rod to both sides should be appropriately increased so that w_1=370 mm.

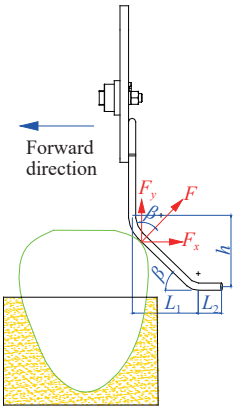

Figure 18 Structural schematic diagram and force analysis of the detection rod

To eliminate the frequent swing of the detection mechanism caused by the small deviation of the beet root and thus avoid frequent jumping of subsequent control signals, the exit width of the detection rod should be designed so that the beet root with the

largest neck but the smallest deviation distance does not contact and collide with the detection rod; that is, the following conditions are met:

$$w_2 \geq 2(L_{dmin}+D_{2max}/2) \tag{2}$$

$$w_2 \leq w_1 \tag{3}$$

where, w_2 is the exit width of the detection rod, mm, and L_{dmin} is the minimum deviation distance of the beet root, mm.

Table 1 lists the agronomic characteristic determination results mentioned above: L_{dmin}=30 mm, D_{2max}=169.01 mm, and w_1= 370 mm. Substituting the above data into Equation (2) yields 229.01 mm ≤ w_2 ≤ 370 mm, where w_2 =240 mm.

To enable the highest unearthed beet root tuber to be detected by the detection rod without hindering its smooth passage, the height of the tilted part of the detection rod (as shown in Figure 18) should meet the following conditions:

$$h \geq H_{2max} \tag{4}$$

where, h is the height of the backward tilt part of the detection rod, mm, and H_{2max} is the maximum unearthed height of the beet root tuber, mm.

Table 2 lists the agronomic characteristic determination results mentioned above; H_{2max}=80 mm. Substituting the above data into Equation (4), h≥80 mm is obtained. To improve the smooth passage of the detection rod, the height of the backward tilt part of the probe rod should be appropriately increased so that h=100 mm.

Force analysis is performed on the detection rod, as shown in Figure 18. Assuming that the force exerted by the sugar beet root on the detection rod is F, to enable the detection rod to move upward and pass smoothly along the surface of the sugar beet root when encountering it, the component force of the force F in the vertical direction should be greater than the component force in the horizontal direction:

$$\begin{cases} F_y \geq F \\ F_y = F\cos\beta \\ F_x = F\sin\beta \end{cases} \tag{5}$$

where, F_y is the vertical component of the force exerted by the sugar beet root on the detection rod, N; F_x is the horizontal component of the force exerted by the sugar beet root on the detection rod, N; and β is the rearward tilt angle of the detection rod, (°).

From Equation (5), $\beta \leq 45°$, and the smaller β is, the more favorable it is for the detection rod to pass over the sugar beet root. However, if β is too small, when the height h of the backward tilt part of the detection rod is constant, the length of the backward tilt part of the detection rod will be too long, which will hinder contact between the two sugar beet roots that are closer to the detection rod. Therefore, the following conditions should be met:

$$L_1+L_2 \leq S_{min} \tag{6}$$

$$L_1=h/\tan\beta \tag{7}$$

where, L_1 is the horizontal length of the backward tilt part of the detection rod, mm; L_2 is the horizontal length of the detection rod, mm; and S_{min} is the minimum plant spacing of sugar beet roots, mm.

Table 2 shows the agronomic characteristic determination results; S_{min} =210 mm. To increase the contact time between the detection rod and the sugar beet root and improve the stability of information detection, L_2=40 mm was used. By substituting the above data into Equations (6) and (7), 30.46° ≤ β ≤ 45° was designed. In summary, β=40° was used, resulting in L_1=119.17 ≈ 119 mm.

4.2 Profiling mechanism

The profiling mechanism is mainly composed of an adjusting bolt, a tension spring, a detection mechanism mounting frame, rotating swing arms, an adjusting sleeve, and an adjusting rod, as shown in Figure 19. The detection mechanism mounting frame is fixedly connected with the adjusting rod. The adjusting rod can be moved up and down in the adjusting sleeve and fixed by the locking bolt. The adjustment sleeve is hinged to the frame through four rotating swing arms. One end of the tension spring is connected to the frame through the adjusting bolt, and the other end is connected to the adjusting sleeve. By adjusting the bolt, the pretension of the tension spring can be adjusted to make the rotating swing arm horizontal. By adjusting the position of the adjusting rod in the adjusting sleeve, the upper and lower initial positions of the detection mechanism can be changed so that the detecting rod fits with the top surface of the ridge without becoming stuck in the soil, preventing the detection of sugar beet roots with lower heights unearthed in the vertical direction. When the detection rod floats up and down along the undulating ridge top surface, it drives the detection mechanism mounting frame and the adjusting sleeve to move up and down around the hinge point of the rotating swing arm, achieving the profiling movement of the detection mechanism. In this way, the coincidence degree of deviation information detection spatial region and sugar beet root growth distribution spatial region in the field can be improved so that agricultural machinery and agronomy can be deeply integrated, and the accuracy of sugar beet root deviation information detection can be improved. The structural optimization of sugar beet harvesting machinery must be closely combined with agronomic characteristics. Wang et al. optimized the structural parameters of the 4TSQ-2 sugar beet top cutter through multi-factor experiments, with the core idea of “improving mechanical structure guided by agronomic parameters”, which is highly consistent with this study.[39]

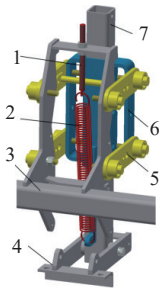

1. Adjusting bolt; 2. Tension spring; 3. Machine frame; 4. Detection mechanism for mounting frame; 5. Rotating swing arm; 6. Adjusting sleeve; 7. Adjusting rod

Figure 19 Structural diagram of the profiling mechanism

5 Performance test

To test the operational performance of the deviation information detection mechanism designed on the basis of agricultural machinery and agronomy integration, it was installed on a traction-type sugar beet combine harvester developed by the Nanjing Institute of Agricultural Mechanization, Ministry of Agriculture and Rural Affairs, and field experiments were conducted in the Chahar Right Front Banner, Ulanqab city, Inner Mongolia Autonomous Region.

5.1 Test materials and instruments

The main test instruments and equipment used include a 4LT-A sugar beet combine harvester, the ridge shape and root distribution detection device developed above, a John Deere 1054 tractor, a 4TGQ-3 sugar beet leaf cutting machine (with a supporting power of 50-70 kW, working width of 1700 mm, 3 rows of operation, and adjustable row spacing of 460-550 mm), a Fastec HiSpec 5 high-speed camera (resolution of 1696×1710, pixel size of 8×8 μm, at 523 frames per second), a HJD-2 digital soil compactor (maximum load of 50 kg, measurement depth of 0-450 mm, accuracy of ±0.5%, and resolution of 0.01 kg), and a TZS-I soil moisture measuring instrument (measurement range of 0-100%, resolution of 0.1%, and relative percentage error ≤ 3%). Other test equipment included benchmarks, tape measures, stopwatches, etc. The test conditions and materials are the same as those in Section 2.1.

5.2 Test methods and indicators

Referring to "JB/T6276-2007 Test Methods for Sugar Beet Harvesting Machinery" and "NY/T 1412-2007 Sugar Beet Harvester Operation Quality", the missed detection rate was selected as the performance evaluation indicator for the deviation information detection mechanism and is defined as follows:

$$\eta_L = N_L/N \times 100\% \quad (8)$$

where, η_L is the missed detection rate, %; N_L is the number of missed detection sugar beet tubers; and N is the total number of sugar beet tubers.

Before the experiment, seven plots with normal sugar beet growth were randomly selected from the field, and samples with a size of 2000×100 cm^2 were randomly selected from each plot. A 4TGQ-3 sugar beet leaf-cutting machine was used to crush the beet leaves and cut off the beet green heads. The deviation information detection mechanism was installed on the 4LT-A sugar beet combine harvester. The high-speed camera was installed on the traction frame at the front end of the combine harvester to monitor the operation of the detection mechanism. Each test time was recorded with a stopwatch, and the average forward speed of the harvester was calculated. The missed detection rate of each sample experiment was analyzed via the high-speed camera, and the experiment was repeated seven times. The soil hardness of the ridge top was determined to be 45-490 kPa (0-5 cm), with a moisture content of 15%-20%. The field test situation is shown in Figure 20.

Figure 20 Field test situation

5.3 Test results and analysis

The performance test results of the deviation information detection mechanism are listed in Table 3.

As shown in Table 3, when the average forward speed of the harvester is 0.84 m/s, the average missed detection rate of the deviation information detection mechanism is 0.56%. When the forward speed of the harvester is 0.54-0.81 m/s, the missed detection rate is 0, indicating that the detection mechanism has high accuracy and good adaptability in detecting sugar beet root tubers growing on single ridges and a high degree of integration of agricultural machinery and agronomy. When the speed of the harvester is 0.93-1.17 m/s, missed detections occur. High-speed photography analysis revealed that when the harvester advanced too fast, individual sugar beet root tubers—which presented smaller root necks and smaller deviation distances but were located between two beet tubers with larger necks, smaller plant spacing, larger deviation distances, and deviation toward the same side—were not detected. This was mainly due to the fast forward speed of the harvester, where the detection rod disengages from a sugar beet root with a large deviation distance; before it can return to its original position, it already contacts another sugar beet root with a large deviation distance and on the same side. In other words, the reset spring stiffness mismatched with the speed. Therefore, the detection rod cannot detect sugar beet roots with a smaller root neck and deviation distance between them, resulting in missed detections.

Table 3 Performance test results of the deviation information detection mechanism

Test number	Forward speed/m·s^{-1}	Missed detection rate η_L/%
1	0.54	0.00
2	0.62	0.00
3	0.73	0.00
4	0.81	0.00
5	0.93	0.95
6	1.05	1.05
7	1.17	1.90
Mean	0.84	0.56

6 Conclusions

1) The agricultural process of mechanized sugar beet production was analyzed; the range of geometric dimensions of typical varieties and planting modes in the main sugar beet production areas, such as the root neck length, root body length, root tail length, large and small diameter of the root neck and root taper, were measured and analyzed; and a three-dimensional geometric model of sugar beet roots was established.

2) A modular and fast splicing ridge shape and root distribution detection device was designed, and agronomic parameters during the harvesting period such as plant spacing, ridge height, unearthed height, and deviation distance were measured and analyzed by the device. A spatial model of the ridge shape and sugar beet root growth distribution on the ridge during the harvesting period was established.

3) A deviation information detection mechanism was designed, and on the basis of agronomic parameter analysis, the structural forms and key parameters of the left-right swing detection mechanism and the up-down floating profiling mechanism were designed. The deep integration of deviation information detection spatial regions and sugar beet tuber field growth distribution spatial regions was realized.

4) Using the missed detection rate as the evaluation indicator, a field performance test was conducted on the deviation information detection mechanism. The results revealed that when the average forward speed of the harvester was 0.84 m/s, the average missed detection rate of the deviation information detection mechanism was 0.56%, indicating high adaptability and detection accuracy. This work provides a foundation for improving the quality and efficiency of automatic row-following correction harvesting operations for sugar beet combine harvesters.

Acknowledgements

This study was supported by the National Natural Science Foundation of China (Grant No. 52105263), Central Government Funds for Guiding Local Scientific and Technological Development (Grant No. 2025ZY0090), and Nanjing Major Science and Technology Special Project (Frontier Technology) (202512115).

[References]

[1] Wang S Y, Gao X M, You Z Y, Peng B L, Wu H C, Hu Z C, et al. Experiment and parameter optimization of an automatic row following system for the traction beet combine harvester. Int J Agric & Biol Eng, 2023; 16(1): 145–152.

[2] Wang F Y, Wang D W. Design and test of 4TSQ-2 sugar beet top cutter. Transactions of the CSAE, 2020; 36(2): 70–78.

[3] Wang S Y, Hu Z C, Chen Y Q, Wu H C, Wang Y Y, et al. Integration of agricultural machinery and agronomy for mechanized peanut production using the vine for animal feed. Biosystems Engineering, 219(2022): 135–152. doi: 10.1016/j.biosystemseng.2022.04.011

[4] Zhang Y Y, Zhang B, Shen C, Liu H L, Huang J C, Tian K P, et al. Review of the field environmental sensing methods based on multi-sensor information fusion technology. Int J Agric & Biol Eng, 2024; 17(2): 1–13.

[5] Marchant W T B, Chittey E T. Automatic control of sugar beet harvester shares. Journal of Agricultural Engineering Research, 1966; 11(3): 188–200.

[6] Billington W P. The design and development of a skew bar topper for sugar beet. Journal of Agricultural Engineering Research. 1984; 29(4): 329–335.

[7] O'Dogherty M J. A geometrical model to define the limits of accuracy of sugar beet topping. Journal of Agricultural Engineering Research, 1986; 35(1): 55–66.

[8] Ivancan S, Sito S, Fabijanic G. Factors of the quality of performance of sugar beet combine harvesters. Die Bodenkultur, 2002; 53(3): 161–166.

[9] Tillett N D, Hague T, Miles S J. Inter-row vision guidance for mechanical weed control in sugar beet. Computers & Electronics in Agriculture, 2002; 33(3): 163–177.

[10] Bulgakov V, Arak M, Boris A, Boris M, Bandura V, Olt J. Experimental study of the distribution of the heights of sugar beet root crowns above the soil surface. Agronomy Research, 2019; 17(6): 2211–2219.

[11] Ospina R, Noguchi N. Simultaneous mapping and crop row detection by fusing data from wide angle and telephoto images. Computers and Electronics in Agriculture, 2019; 162(7): 602–612.

[12] Tsukor V, Strothmann W, Schwamm W, Ruckelshausen A. Contactless sensor system for row navigation and automatic depth control for a sugar beet harvester using a 3D time of flight (ToF) camera. Word Conference on Computers in Agriculture and Natural Resources, San Jose Costa Rica, Paper Book, 2014; pp.1–8.

[13] Yang L L, Xu Y Y, Liang Y J, Qin J, Li Y B, Wang X X, et al. Extraction of straight field roads between farmlands based on agricultural vehicle-mounted LiDAR. Int J Agric & Biol Eng, 2022; 15(5): 155–162.

[14] Ivanetz G, Ovsyanko V, Vyrski A. Computer modeling of beet harvester digging bodies-soil interaction. Journal of Research & Applications in Agricultural Engineering, 2007; 52(1): 8–12.

[15] Bulgakov V, Adamchuk V, Arak M, Olt J. A theoretical study of haulm loss resulting from rotor topper oscillation. Chemical Engineering Transactions, 2017; 58: 223–228.

[16] Bulgakov V, Adamchuk V, Nozdrovicky L, Ihnatiev Y. Theory of vibrations of sugar beet leaf harvester front-mounted on universal tractor. Acta Technologica Agriculturae, 2017; 4: 96–103.

[17] Pádua L, Chojka A, Morais R, Peres E, Sousa J J. Versatile method for grapevine row detection in challenging vineyard terrains using aerial imagery. Computers and Electronics in Agriculture, 2024; 226: 109372.

[18] Biglia A, Zaman S, Gay P, Aimonino D R, Comba L. 3D point cloud density-based segmentation for vine rows detection and localization. Computers and Electronics in Agriculture, 2022; 199: 107166.

[19] Bah M D, Hafiane A, Canals R. Hierarchical graph representation for unsupervised crop row detection in images. Expert Systems with Applications, 2023; 216; 119478. doi: 10.1016/j.eswa.2022.119478

[20] Visentin F, Cremasco S, Sozzi M, Signorini L, Signorini M, Marinello F, Muradore R. A mixed-autonomous robotic platform for intra-row and inter-row weed removal for precision agriculture. Computers and Electronics in Agriculture, 2023; 214: 108270.

[21] Rocha B M, Fonseca A U, Pedrini H, Soares F. Automatic detection and evaluation of sugarcane planting rows in aerial images. Information Processing in Agriculture, 2023; 10: 400–415.

[22] Wang S Y, Hu Z C, Peng B L, Wu H C, Gu F W, Wang H O. Simulation of auto-follow row detection mechanism in beet harvester based on ADAMS. Transactions of the CSAM, 2013; 44(12): 62–67.

[23] Wang S Y, Hu Z C, Wu H C, Peng B L, Xie H X, Gu F W. Design and test of hydraulic correction execution system in automated row-followed for beet harvester. Agricultural Mechanization Research, 2016; 38(3): 155–162.

[24] Wang F Y, Zhang D X. Parameter optimization and test on auto guide device for disc type sugar beet harvester. Transactions of the CSAE, 2015; 31(8): 27–33.

[25] Wang F Y, Zhang Z Y, Zhang Q, Wang X. Design optimization and experiment of tooth-plate topping device of sugar beet harvester. Transactions of the CSAM, 2020; 51(11): 168–175.

[26] Wang S Y, Hu Z C, Chen C, Gao X M, Gu F W, Wu H C. Bench test and analysis on performance of autofollow row for traction sugar beet combine harvester. Transactions of the CSAM, 2020; 51(4): 103–112, 163.

[27] Yang R B, Shang S Q, Wang J S, Li X C. Research on auto-follow row technology employed in root-tuber crops harvester. 2011 Annual Conference of CSAE, Chongqing, 2011; pp.138–142.

[28] Hu Y, Zhang K L, Xu L M. Boundary detection for corn combine harvester's auto-follow row system based on laser radar. 2018 ASABE Annual International Meeting, Detroit, 2018; pp.576–582.

[29] Li T, Zhou J, Xu W Y, Zhang H, Liu C G, Jiang W. Design and test of auto-follow row system employed in root and stem crops harvester. Transactions of the CSAM, 2013; 50(11): 102–110

[30] Han X Z, Kim H J, Chan W J, Hee C M, Jung H K, Sang Y Y. Application of a 3D tractor-driving simulator for slip estimation-based path-tracking control of auto-guided tillage operation. Biosystems Engineering, 2019; 178(2): 70–85.

[31] Zhang K L, Hu Y, Yang L, Zhang D X, Cui T, Fan L L. Design and experiment of auto-follow row system for corn harvester. Transactions of the CSAM, 2020; 51(2): 103–114.

[32] Ma Z H, Tao Z Y, Du X Q, Yu Y X, Wu C Y. Automatic detection of crop root rows in paddy fields based on straight-line clustering algorithm and supervised learning method. Biosystems Engineering, 2021; 211: 63–76.

[33] Ruan Z W, Chang P H, Cui S Q, Luo J Q, Gao R, Su Z B. A precise crop row detection algorithm in complex farmland for unmanned agricultural machines. Biosystems Engineering, 2023; 232: 1–12.

[34] Li D F, Li B L, Long S F, Feng H Q, Xi T, Kang S, Wang J. Rice seedling row detection based on morphological anchor points of rice stems. Biosystems Engineering, 2023; 226: 71–85.

[35] Diao Z H, Guo P L, Zhang B H, Zhang D Y, Yan J N, He Z D, et al. Maize crop row recognition algorithm based on improved UNet network. Computers and Electronics in Agriculture, 2023; 210: 107940.

[36] Luo Y S, Wei L L, Xu L Z, Zhang Q, Liu J Y, Cai Q B, Zhang W B. Stereo-vision-based multi-crop harvesting edge detection for precise automatic steering of combine harvester. Biosystems Engineering, 2022; 215: 115–128.

[37] Wu H C, Hu Z C, Peng B L, Gu F W, Wang H O, Wang B K. Development of auto-follow row system employed in pull-type beet combine harvester. Transactions of the CSAE, 2013; 29(12): 17–24.

[38] Gu F W, Hu Z C, Wu H C, Peng B L, Gao X M, Wang S Y. Development and experiment of 4LT-A staggered-dig sugar beet combine. Transactions of the CSAE, 2014; 30(23): 1–9.

[39] Wang F Y, Zhang Z Y, Pan Y F, Yun Y L, Wang D W. Optimized design of the 4TSQ-2 sugar beet top cutting machine. Int J Agric & Biol Eng, 2022; 15(2): 111–116.